Aerospace Science and Technology 39 (2014) 260–271

Contents lists available at ScienceDirect

Aerospace Science and Technology

www.elsevier.com/locate/aescte

Large deflection analysis of moderately thick radially functionally graded annular sector plates fully and partially rested on two-parameter elastic foundations by GDQ method

Farhad Alinaghizadeh, Mehran Kadkhodayan *

Ferdowsi University of Mashhad, Department of Mechanical Engineering, Mashhad, Iran

ARTICLE INFO

Article history:
Received 1 July 2013
Received in revised form 30 May 2014
Accepted 17 September 2014
Available online 18 October 2014

Keywords:
Sector plate
Non-linear bending analysis
Pasternak foundation strips
Generalized differential quadrature
Functionally graded material

ABSTRACT

This paper presents an investigation into large deflection analysis of moderately thick radially functionally graded (RFG) annular sector plates fully and partially rested on two-parameter (Pasternak) elastic foundation by employing Generalized Differential Quadrature (GDQ) method. The material properties are graded through the radial direction of plates according to a power-law distribution of the volume fraction of the constituent. Based on the first-order shear deformation theory in conjunction with non-linear von Kármán assumptions, the equilibrium equations are derived. Application of GDQ method to the equilibrium equations leads to a system of non-linear algebraic equations. The set of non-linear algebraic equations are then solved by employing the Newton–Raphson iterative scheme. It is shown that the predictions of GDQ method vis-à-vis other numerical methods reported in the literature, are in a good agreement. Furthermore, effects of change in power law index, geometrical parameters and stiffness of foundation are studied in detail.

1. Introduction

Analysis of plates and shells made of functionally graded materials (FGMs) has become famous among researchers since their introduction in 1984 by a group of material scientists in Japan [32]. Material properties of FGMs vary continuously in at least one direction according to a specific profile. These materials are typically made of ceramic and metal. The ceramic component enables the material to withstand high-temperature environments due to its low thermal conductivity and the ductile metal component precludes fracture.

An analytical closed form solution is not always obtainable therefore several semi-analytical and numerical methods have been presented. Among them one may refer to the GDQ method which is a numerical method with high accuracy even by employing a few numbers of grid points. The main advantage of the GDQ method vis-à-vis its classical version differential quadrature method (DQM) [5], is that the weighting coefficients are readily obtained without restrictions on the choice of grid points.

Circular and annular sector plates have numerous applications in industrial fields. Nevertheless, studies on annular sector plates are rare compared to those available on rectangular plates. Large deflection analysis of moderately thick annular sector plates is presented by Salehi and Shahidi [29] using dynamic relaxation (DR) method. Nath et al. [23] studied non-linear bending analysis of moderately thick annular sector plates using Chebyshev polynomials. Aghdam et al. [1] used extended Kantorovich method (EKM) to obtain solutions for bending analysis of thin fully clamped annular sector plates subjected to uniform and non-uniform load. In another work of Aghdam et al. [2] bending analysis of moderately thick FG annular sector plates was carried out using EKM in conjunction with GDQ method. Andakhshideh et al. [3] employed GDQ method to study non-linear bending of laminated annular sector plates with any combination of boundary conditions. Some researchers also studied RFG annular sector plates. Mousavi and Tahani [21] presented EKM solutions for moderately thick RFG annular sector plates. Recently, Fereidoon et al. [10] investigated small deflection of thin RFG annular sector plates using EKM. Hejripour and Saidi [15] studied non-linear free vibration analysis of moderately thick annular sector plates by DQM. Saidi et al. [28] presented analytical solutions for bending of thin FG annular sector plates. On the basis of the Reddy's third-order shear deformation theory, bending [4], buckling [14], and free vibration [9] of annular sector plates have been carried out.

Several attempts have been made to model an actual foundation. Winkler foundation is simplest and most widely used model. This model represents a continuous elastic foundation as closely

* Corresponding author.
E-mail addresses: Farhad.Alinaghi.zadeh@gmail.com (F. Alinaghizadeh), kadkhoda@um.ac.ir (M. Kadkhodayan).

http://dx.doi.org/10.1016/j.ast.2014.09.014
1270-9638/

spaced, linear, separate springs. To modify the Winkler model, several two-parameter models such as Pasternak model are proposed. In this model the springs of Winkler model are assumed to attach to a plate consist of incompressible vertical elements which can deform only by transverse shear.

Studies on rectangular plates resting on Winkler or Pasternak foundations have attracted the attention of many researchers. Kobayashi and Sonoda [18] presented Levy-type solutions for bending analysis of moderately thick square plates resting on Winkler foundation. Liew et al. [19] studied moderately thick square plates resting on Winkler foundation employing DQM. Using the DQ method, bending analysis of moderately thick square plates rested on two-parameter foundation was performed by Han and Liew [13]. Liu [20] employed differential quadrature element method to analyze bending response of moderately thick square plates on Winkler foundation with any combination of boundary conditions and various sorts of loadings.

As per the review of literature it appears that although numerous studies on bending analysis of rectangular plates resting on foundation are available, but very few studies on analysis of annular sector plates resting on foundation have been carried out. Naderi and Saidi [22] presented an analytical solution for buckling analysis of moderately thick FG annular sector plates resting on Winkler foundation. Hosseini-Hashemi et al. [16] investigated buckling of RFG thin annular sector plates resting on Pasternak elastic foundation using DQM. In another work of Hosseini-Hashemi et al. [17] vibration analysis of variable thickness RFG annular sector plates on elastic foundation was carried out.

Apart from Nobakhti and Aghdam [25] that studied thick rectangular plates partially rested on foundation, all previous studies in the literature are confined to plates completely resting on foundation. However, plates partially rested on foundation have a wide range of applications in industry, i.e., plates that are employed to cover holes or cavities in structures. Thus far the authors have not encountered any paper dealing with large deflection analysis of RFG annular sector plates as well as bending analysis of annular sector plates on foundation. Particular interest of the present study is large deflection analysis of RFG annular sector plates fully and partially rested on Pasternak foundation.

In the present paper, non-linear bending analysis of RFG annular sector plates resting on Pasternak foundations or stripes is presented. By employing the principle of minimum total potential energy the equilibrium equations are obtained based on the first-order shear deformation theory (FSDT) and von Kármán type non-linearity. The GDQ method in conjunction with the Newton–Raphson iterative scheme is then used to solve the set of five nonlinear equilibrium equations. A comparison study is carried out and validity and accuracy of the results are demonstrated. Furthermore, the influences produced by geometrical parameters, power law index and stiffness of the foundation are studied in detail.

2. Theoretical formulation

2.1. Geometry and material properties

An annular sector plate with inner radius r_i outer radius r_o constant thickness h and total angle α subjected to a uniform pressure P_z rested on Pasternak elastic foundation is considered. The normal and shear coefficients of the Pasternak foundation are k_f and g_f, respectively. The Pasternak foundation model can become the Winkler foundation model by assuming $g_f = 0$. In addition, problem can be extended to a plate partially rested on foundation i.e., portions of the plate along edges are rested on foundation, and there is no foundation at the middle of the plate. The portions of the plate on foundation along circumferential edges and radial edges are specified by t and τ, respectively. The geometry of the plate, coordinate system and the portions of the plate with and without foundation are shown in Figs. 1 and 2.

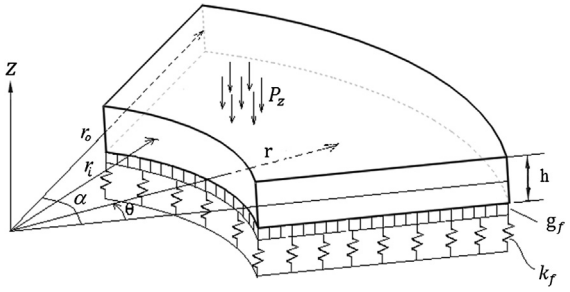

Fig. 1. Geometry and coordinate system of an annular sector plate resting on Pasternak foundation.

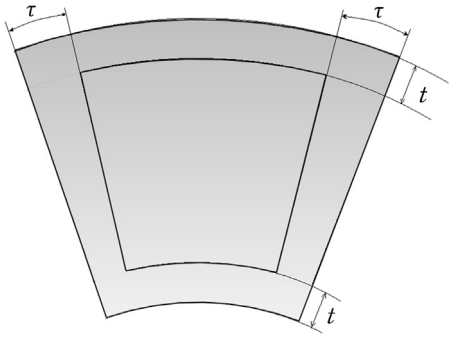

Fig. 2. RFG annular sector plate partially rested on foundation.

It is assumed that the material properties of the FGM plates vary continuously in radial direction according to a power-law function. Therefore, the Young's modulus and Poisson's ratio can be expressed as follows [21]:

$$E(r) = (E_c - E_m)\left(\frac{r - r_i}{r_o - r_i}\right)^n + E_m,$$
$$\nu(r) = (\nu_c - \nu_m)\left(\frac{r - r_i}{r_o - r_i}\right)^n + \nu_m, \tag{1}$$

where c and m refer to the ceramic and metal constituents, respectively and n denotes the power-law index and is equal or greater than zero. It is obvious from Eq. (1) that the inner surface ($r = r_i$) of the plate is metal-rich and the outer surface ($r = r_o$) is purely ceramic. Furthermore, when n is zero or takes a very large value the plate material is homogeneous and completely ceramic or metal, respectively.

2.2. Equilibrium equations

The displacement field of the plate based upon the first order shear deformation theory in polar coordinate is given as [27]:

$$U(r,\theta,z) = u(r,\theta) + z\phi_r(r,\theta),$$
$$V(r,\theta,z) = v(r,\theta) + z\phi_\theta(r,\theta),$$
$$W(r,\theta,z) = w(r,\theta), \tag{2}$$

where U, V and W are displacement fields related to r, θ and z directions, respectively. Furthermore, u, v and w indicate the displacement component of a point at the middle surface (i.e., $z = 0$) of the plate along r, θ and z directions, respectively, also ϕ_r and ϕ_θ denote rotation about the θ- and r-axes, respectively. By introducing the displacement field (2) into the von Kármán non-linear strain-displacement equations [12] strain components are found as follows:

$$\varepsilon_r = \frac{\partial u}{\partial r} + \frac{1}{2}\left(\frac{\partial w}{\partial r}\right)^2 + z\frac{\partial \phi_r}{\partial r},$$
$$\varepsilon_\theta = \frac{1}{r}\left(\frac{\partial v}{\partial \theta} + u\right) + \frac{1}{2r^2}\left(\frac{\partial w}{\partial \theta}\right)^2 + \frac{z}{r}\left(\frac{\partial \phi_\theta}{\partial \theta} + \phi_r\right),$$
$$\varepsilon_z = 0,$$
$$2\varepsilon_{r\theta} = \frac{\partial v}{\partial r} + \frac{1}{r}\frac{\partial u}{\partial \theta} - \frac{v}{r} + \frac{1}{r}\frac{\partial w}{\partial r}\frac{\partial w}{\partial \theta} + z\left(\frac{\partial \phi_\theta}{\partial r} + \frac{1}{r}\frac{\partial \phi_r}{\partial \theta} - \frac{\phi_\theta}{r}\right),$$
$$2\varepsilon_{rz} = \frac{\partial w}{\partial r} + \phi_r,$$
$$2\varepsilon_{\theta z} = \frac{1}{r}\frac{\partial w}{\partial \theta} + \phi_\theta. \tag{3}$$

Employing the principle of minimum total potential energy [26] the equilibrium equations are obtained as:

$$\delta u: \quad \frac{\partial N_r}{\partial r} + \frac{1}{r}\frac{\partial N_{r\theta}}{\partial \theta} + \frac{N_r - N_\theta}{r} = 0,$$
$$\delta v: \quad \frac{\partial N_{r\theta}}{\partial r} + \frac{1}{r}\frac{\partial N_\theta}{\partial \theta} + \frac{2}{r}N_{r\theta} = 0,$$
$$\delta w: \quad \frac{\partial Q_r}{\partial r} + \frac{1}{r}\frac{\partial Q_\theta}{\partial \theta} + \frac{1}{r}Q_r + N_1 - k_f w + g_f \nabla^2 w = P_z,$$
$$\delta \phi_r: \quad \frac{\partial M_r}{\partial r} + \frac{\partial M_{r\theta}}{r\partial \theta} + \frac{M_r - M_\theta}{r} - Q_r = 0,$$
$$\delta \phi_\theta: \quad \frac{\partial M_{r\theta}}{\partial r} + \frac{\partial M_\theta}{r\partial \theta} + \frac{2}{r}M_{r\theta} - Q_\theta = 0, \tag{4}$$

in which,

$$N_1 = N_r\frac{\partial^2 w}{\partial r^2} + N_\theta\left(\frac{1}{r}\frac{\partial w}{\partial r} + \frac{1}{r^2}\frac{\partial^2 w}{\partial \theta^2}\right) + 2N_{r\theta}\left(\frac{1}{r}\frac{\partial^2 w}{\partial r \partial \theta} - \frac{1}{r^2}\frac{\partial w}{\partial \theta}\right). \tag{5}$$

Furthermore, in the third equilibrium equation ∇^2 is the Laplacian operator in polar coordinate. The stress and moment resultants in (4) and (5) are defined as follows:

$$(N_r, N_\theta, N_{r\theta}) = \int_{-h/2}^{h/2} (\sigma_r, \sigma_\theta, \sigma_{r\theta})dz,$$
$$(Q_r, Q_\theta) = K^2 \int_{-h/2}^{h/2} (\sigma_{rz}, \sigma_{\theta z})dz,$$
$$(M_r, M_\theta, M_{r\theta}) = \int_{-h/2}^{h/2} z(\sigma_r, \sigma_\theta, \sigma_{r\theta})dz, \tag{6}$$

where K^2 is the shear correction factor which is considered to be 5/6 [24]. Considering plane-stress state for the RFG annular sector plate, the stresses are defined as:

$$\sigma_r = \frac{E(r)}{1-\nu(r)^2}\left(\varepsilon_r + \nu(r)\varepsilon_\theta\right),$$
$$\sigma_\theta = \frac{E(r)}{1-\nu(r)^2}\left(\varepsilon_\theta + \nu(r)\varepsilon_r\right),$$
$$\sigma_{r\theta} = \frac{E(r)}{2(1+\upsilon(r))}(2\varepsilon_{r\theta}),$$
$$\sigma_{rz} = \frac{E(r)}{2(1+\upsilon(r))}(2\varepsilon_{rz}),$$
$$\sigma_{\theta z} = \frac{E(r)}{2(1+\upsilon(r))}(2\varepsilon_{\theta z}). \tag{7}$$

Substituting Eqs. (1) and (3) into Eq. (7) and the subsequent results into Eq. (6), the stress and moment resultants are written in terms of displacements and rotations as follows:

$$\{F\} = [C]\{U\}, \tag{8}$$

in which

$$\{F\} = \{N_r, N_\theta, N_{r\theta}, M_r, M_\theta, M_{r\theta}, Q_r, Q_\theta\}^T, \tag{9a}$$

$$[C] = \begin{bmatrix} A_{11} & A_{12} & 0 & 0 & 0 & 0 & 0 & 0 \\ A_{12} & A_{11} & 0 & 0 & 0 & 0 & 0 & 0 \\ 0 & 0 & A_{33} & 0 & 0 & 0 & 0 & 0 \\ 0 & 0 & 0 & D_{11} & D_{12} & 0 & 0 & 0 \\ 0 & 0 & 0 & D_{12} & D_{11} & 0 & 0 & 0 \\ 0 & 0 & 0 & 0 & 0 & D_{33} & 0 & 0 \\ 0 & 0 & 0 & 0 & 0 & 0 & A_{33} & 0 \\ 0 & 0 & 0 & 0 & 0 & 0 & 0 & A_{33} \end{bmatrix}, \tag{9b}$$

$$\{U\} = \begin{Bmatrix} \partial u/\partial r + (\partial w/\partial r)^2/2 \\ \partial v/r\partial\theta + u/r + (\partial w/r\partial\theta)^2/2 \\ \partial u/r\partial\theta + \partial v/\partial r - v/r + (\partial w/\partial r)(\partial w/r\partial\theta) \\ \partial\phi_r/\partial r \\ \partial\phi_\theta/r\partial\theta + \phi_r/r \\ \partial\phi_r/r\partial\theta + \partial\phi_\theta/\partial r - \phi_\theta/r \\ K^2(\phi_r + \partial w/\partial r) \\ K^2(\phi_\theta + \partial w/r\partial\theta) \end{Bmatrix}. \tag{9c}$$

The coefficients in (9b) are defined as:

$$(A_{11}, D_{11}) = \frac{E(r)}{1-\nu(r)^2}\left(h, \frac{h^3}{12}\right),$$
$$(A_{12}, D_{12}) = \frac{E(r)\nu(r)}{1-\nu(r)^2}\left(h, \frac{h^3}{12}\right),$$
$$(A_{33}, D_{33}) = \frac{E(r)}{2(1+\nu(r))}\left(h, \frac{h^3}{12}\right). \tag{10}$$

Upon substitution of Eq. (8) into Eq. (4), the ultimate form of equilibrium equations can be obtained as:

$$A_{11}\frac{\partial^2 u}{\partial r^2} + \frac{A_{33}}{r^2}\frac{\partial^2 u}{\partial \theta^2} + \left(\frac{dA_{11}}{dr} + \frac{A_{11}}{r}\right)\frac{\partial u}{\partial r} + \left(\frac{1}{r}\frac{dA_{12}}{dr} - \frac{A_{11}}{r^2}\right)u + \left(\frac{A_{33}}{r} + \frac{A_{12}}{r}\right)\frac{\partial^2 v}{\partial r \partial \theta} + \left(\frac{1}{r}\frac{dA_{12}}{dr} - \frac{A_{11}}{r^2} - \frac{A_{33}}{r^2}\right)\frac{\partial v}{\partial \theta} + \frac{1}{2}\left(\frac{dA_{11}}{dr} + \frac{A_{11}}{r} - \frac{A_{12}}{r}\right)\left(\frac{\partial w}{\partial r}\right)^2 + \frac{1}{2}\left(\frac{1}{r^2}\frac{dA_{12}}{dr} - \frac{A_{11}}{r^3} - \frac{A_{12}}{r^3}\right)\left(\frac{\partial w}{\partial \theta}\right)^2 + A_{11}\frac{\partial w}{\partial r}\frac{\partial^2 w}{\partial r^2} + \frac{A_{33}}{r^2}\frac{\partial w}{\partial r}\frac{\partial^2 w}{\partial \theta^2} + \left(\frac{A_{33}}{r^2} + \frac{A_{12}}{r^2}\right)\frac{\partial w}{\partial \theta}\frac{\partial^2 w}{\partial r \partial \theta} = 0, \tag{11a}$$

$$\left(\frac{A_{33}}{r} + \frac{A_{12}}{r}\right)\frac{\partial^2 u}{\partial r \partial \theta} + \left(\frac{1}{r}\frac{dA_{33}}{dr} + \frac{A_{11}}{r^2} + \frac{A_{33}}{r^2}\right)\frac{\partial u}{\partial \theta} + A_{33}\frac{\partial^2 v}{\partial r^2} + \frac{A_{11}}{r^2}\frac{\partial^2 v}{\partial \theta^2} + \left(\frac{dA_{33}}{dr} + \frac{A_{33}}{r}\right)\frac{\partial v}{\partial r} + \left(-\frac{1}{r}\frac{dA_{33}}{dr} - \frac{A_{33}}{r^2}\right)v + \left(\frac{A_{12}}{r} + \frac{A_{33}}{r}\right)\frac{\partial w}{\partial r}\frac{\partial^2 w}{\partial r \partial \theta} + \frac{A_{33}}{r}\frac{\partial^2 w}{\partial r^2}\frac{\partial w}{\partial \theta} + \left(\frac{1}{r}\frac{dA_{33}}{dr} + \frac{A_{33}}{r^2}\right)\frac{\partial w}{\partial \theta}\frac{\partial w}{\partial r} + \frac{A_{11}}{r^3}\frac{\partial^2 w}{\partial \theta^2}\frac{\partial w}{\partial \theta} = 0, \tag{11b}$$

$$A_{33}K^2\frac{\partial^2 w}{\partial r^2}+\frac{A_{33}}{r^2}K^2\frac{\partial^2 w}{\partial\theta^2}+\left(\frac{dA_{33}}{dr}+\frac{A_{33}}{r}\right)K^2\frac{\partial w}{\partial r}-k_f w + g_f\left(\frac{\partial^2 w}{\partial r^2}+\frac{1}{r}\frac{\partial w}{\partial r}+\frac{1}{r^2}\frac{\partial^2 w}{\partial\theta^2}\right)+A_{33}K^2\frac{\partial\phi_r}{\partial r}+\frac{A_{33}}{r}K^2\phi_r + \frac{dA_{33}}{dr}K^2\phi_r+\frac{A_{33}}{r}K^2\frac{\partial\phi_\theta}{\partial\theta}+2\frac{A_{33}}{r^2}\frac{\partial w}{\partial\theta}\frac{\partial w}{\partial r}\frac{\partial^2 w}{\partial r\partial\theta} + \frac{A_{12}}{2r}\left(\frac{\partial w}{\partial r}\right)^3+\frac{A_{11}}{2}\frac{\partial^2 w}{\partial r^2}\left(\frac{\partial w}{\partial r}\right)^2+\frac{A_{12}}{2r^2}\frac{\partial^2 w}{\partial r^2}\left(\frac{\partial w}{\partial\theta}\right)^2 + \frac{A_{12}}{2r^2}\frac{\partial^2 w}{\partial\theta^2}\left(\frac{\partial w}{\partial r}\right)^2+\left(\frac{A_{11}}{2r^3}-2\frac{A_{33}}{r^3}\right)\left(\frac{\partial w}{\partial\theta}\right)^2\frac{\partial w}{\partial r} + \frac{A_{11}}{2r^4}\frac{\partial^2 w}{\partial\theta^2}\left(\frac{\partial w}{\partial\theta}\right)^2+2\frac{A_{33}}{r^2}\frac{\partial^2 w}{\partial r\partial\theta}\frac{\partial u}{\partial\theta}+A_{11}\frac{\partial^2 w}{\partial r^2}\frac{\partial u}{\partial r} + \frac{A_{12}}{r}\frac{\partial w}{\partial r}\frac{\partial u}{\partial r}+\frac{A_{12}}{r^2}\frac{\partial^2 w}{\partial\theta^2}\frac{\partial u}{\partial r}-2\frac{A_{33}}{r^3}\frac{\partial w}{\partial\theta}\frac{\partial u}{\partial\theta}+\frac{A_{12}}{r}\frac{\partial^2 w}{\partial r^2}u + \frac{A_{11}}{r}\frac{\partial w}{\partial r}u+\frac{A_{11}}{r^3}\frac{\partial^2 w}{\partial\theta^2}u+2\frac{A_{33}}{r}\frac{\partial^2 w}{\partial r\partial\theta}\frac{\partial v}{\partial r}-2\frac{A_{33}}{r^2}\frac{\partial w}{\partial\theta}\frac{\partial v}{\partial r} + \frac{A_{12}}{r}\frac{\partial^2 w}{\partial r^2}\frac{\partial v}{\partial\theta}+\frac{A_{11}}{r^2}\frac{\partial w}{\partial r}\frac{\partial v}{\partial\theta}+\frac{A_{11}}{r^3}\frac{\partial^2 w}{\partial\theta^2}\frac{\partial v}{\partial\theta}-2\frac{A_{33}}{r^2}\frac{\partial^2 w}{\partial r\partial\theta}v + 2\frac{A_{33}}{r^3}\frac{\partial w}{\partial\theta}v=P_z, \tag{11c}$$

$$\left(\frac{D_{33}}{r}+\frac{D_{12}}{r}\right)\frac{\partial^2\phi_\theta}{\partial r\partial\theta}+\left(\frac{-D_{33}}{r^2}-\frac{D_{11}}{r^2}+\frac{1}{r}\frac{dD_{12}}{dr}\right)\frac{\partial\phi_\theta}{\partial\theta} + D_{11}\frac{\partial^2\phi_r}{\partial r^2}+\left(\frac{dD_{11}}{dr}+\frac{D_{11}}{r}\right)\frac{\partial\phi_r}{\partial r} + \frac{D_{33}}{r^2}\frac{\partial^2\phi_r}{\partial\theta^2}\left(\frac{1}{r}\frac{dD_{12}}{dr}-\frac{D_{11}}{r^2}-A_{33}K^2\right)\phi_r - A_{33}K^2\frac{\partial w}{\partial r}=0, \tag{11d}$$

$$\left(\frac{D_{33}}{r}+\frac{D_{12}}{r}\right)\frac{\partial^2\phi_r}{\partial r\partial\theta}+\left(\frac{D_{33}}{r^2}+\frac{D_{11}}{r^2}+\frac{1}{r}\frac{dD_{33}}{dr}\right)\frac{\partial\phi_r}{\partial\theta} + D_{33}\frac{\partial^2\phi_\theta}{\partial r^2}+\left(\frac{dD_{33}}{dr}+\frac{D_{33}}{r}\right)\frac{\partial\phi_\theta}{\partial r} + \frac{D_{11}}{r^2}\frac{\partial^2\phi_\theta}{\partial\theta^2}\left(-\frac{1}{r}\frac{dD_{33}}{dr}-\frac{D_{33}}{r^2}-A_{33}K^2\right)\phi_\theta - \frac{A_{33}}{r}K^2\frac{\partial w}{\partial\theta}=0. \tag{11e}$$

The system of five non-linear partial differential equations is solved in conjunction with the following clamped boundary and simply supported conditions:

(a) On the radial edges
Clamped:

$$u=v=w=\phi_r=\phi_\theta=0, \tag{12}$$

Simply supported:

$$u=v=w=\phi_r=M_\theta=0, \tag{13}$$

(b) On the circumferential edges
Clamped:

$$u=v=w=\phi_r=\phi_\theta=0, \tag{14}$$

Simply supported:

$$u=v=w=M_r=\phi_\theta=0. \tag{15}$$

2.3. Application of the GDQ method

In this part a review of the GDQ method is outlined, more detail of DQM and its developments can be found in [6,31,30]. In the GDQ method the partial derivative of a function with respect to a variable at a specific grid point is approximated as a weighted linear sum of the function values at all discrete points in the complete domain of that variable. In order to clarify the concept, a one dimensional function $f(x)$ on a domain $a\le x\le b$ which is discretized by N grid points is considered. The mth-order differential of the function at an arbitrary grid point x_i is given by:

$$\left.\frac{d^m f(x)}{dx^m}\right|_{x=x_i}=\sum_{j=1}^{N}C_{ij}^{(m)}f(x_j),\quad i=1,2,\ldots,N \tag{16}$$

where $C_{ij}^{(m)}$ are the weighting coefficients, and for the first order derivative are calculated by:

$$C_{ij}^{(1)}=\frac{M^{(1)}(x_i)}{(x_i-x_j)M^{(1)}(x_j)},\quad i,j=1,2,\ldots,N \tag{17}$$

where

$$M^{(1)}(x_k)=\prod_{j=1(j\neq k)}^{N}(x_k-x_j). \tag{18}$$

Eq. (17) is used for $i\neq j$, the rest of weighting coefficients are obtained by:

$$C_{ii}^{(1)}=-\sum_{j=1(j\neq i)}^{N}C_{ij}^{(1)},\quad i=1,2,\ldots,N \tag{19}$$

Furthermore, the following recurrence formula is used to obtain weighting coefficients of second- and higher-order derivatives:

$$C_{ij}^{(m)}=m\left[C_{ij}^{(1)}C_{ii}^{(m-1)}-\frac{C_{ij}^{(m-1)}}{x_i-x_j}\right], \tag{20}$$

Eq. (20) is employed for $i\neq j$, $i,j=1,2,\ldots,N$ and $m=2,3,\ldots,N-1$. The rest of weighting coefficients are calculated by:

$$C_{ii}^{(m)}=-\sum_{j=1(j\neq i)}^{N}C_{ij}^{(m)}, \tag{21}$$

where $i=1,2,\ldots,N$ and $m=2,3,\ldots,N-1$.

The accuracy of the method depends on numbers of grid points as well as positions of them. It is found that one of the best choices for obtaining grid points is the roots of Chebyshev polynomials as:

$$x_i=\frac{1}{2}\left[a+b+(a-b)\cos\left(\frac{(i-1)\pi}{N-1}\right)\right],\quad i=1,2,\ldots,N \tag{22}$$

To solve the problem, the equilibrium equations in terms of displacements and rotations are re-written in discretized algebraic form according to GDQ method. The discretized form of the first equilibrium equation is obtained as:

$$A_{11}|_{r=r_i}\left(\sum_{k=1}^{N_r}B_{ik}u(k,j)\right)+\left.\frac{A_{33}}{r^2}\right|_{r=r_i}\left(\sum_{k=1}^{N_\theta}\overline{B_{jk}}u(i,k)\right) + \left.\left(\frac{dA_{11}}{dr}+\frac{A_{11}}{r}\right)\right|_{r=r_i}\left(\sum_{k=1}^{N_r}A_{ik}u(k,j)\right) + \left.\left(\frac{1}{r}\frac{dA_{12}}{dr}-\frac{A_{11}}{r^2}\right)\right|_{r=r_i}u(i,j)$$

$$+\left(\frac{A_{33}}{r}+\frac{A_{12}}{r}\right)\Big|_{r=r_i}\left(\sum_{k=1}^{N_r}A_{ik}\sum_{m=1}^{N_\theta}\overline{A_{jm}}v(k,m)\right)$$
$$+\left(\frac{1}{r}\frac{dA_{12}}{dr}-\frac{A_{11}}{r^2}-\frac{A_{33}}{r^2}\right)\Big|_{r=r_i}\left(\sum_{k=1}^{N_\theta}\overline{A_{jk}}v(i,k)\right)$$
$$+\frac{1}{2}\left(\frac{dA_{11}}{dr}+\frac{A_{11}}{r}-\frac{A_{12}}{r}\right)\Big|_{r=r_i}\left(\sum_{k=1}^{N_r}A_{ik}w(k,j)\right)^2$$
$$+\frac{1}{2}\left(\frac{1}{r^2}\frac{dA_{12}}{dr}-\frac{A_{11}}{r^3}-\frac{A_{12}}{r^3}\right)\Big|_{r=r_i}\left(\sum_{k=1}^{N_\theta}\overline{A_{jk}}w(i,k)\right)^2$$
$$+A_{11}|_{r=r_i}\left(\sum_{k=1}^{N_r}A_{ik}w(k,j)\right)\left(\sum_{k=1}^{N_r}B_{ik}w(k,j)\right)$$
$$+\frac{A_{33}}{r^2}\Big|_{r=r_i}\left(\sum_{k=1}^{N_r}A_{ik}w(k,j)\right)\left(\sum_{k=1}^{N_\theta}\overline{B_{jk}}w(i,k)\right)$$
$$+\left(\frac{A_{33}}{r^2}+\frac{A_{12}}{r^2}\right)\Big|_{r=r_i}\left(\sum_{k=1}^{N_\theta}\overline{A_{jk}}w(i,k)\right)$$
$$\times\left(\sum_{k=1}^{N_r}A_{ik}\sum_{m=1}^{N_\theta}\overline{A_{jm}}w(k,m)\right)=0, \tag{23}$$

where $i=1,2,\ldots,N_r$ and $j=1,2,\ldots,N_\theta$. Furthermore, A_{pq} and $\overline{A_{pq}}$, denote weighting coefficients for first order derivative with respect to r and θ, respectively, and B_{pq} and $\overline{B_{pq}}$, are weighting coefficients of second order derivative with respect to r and θ, respectively.

The remaining equilibrium equations are discretized in an analogous manner. The discretization of the five equilibrium equations leads to a system of $5(N_r\times N_\theta)$ non-linear algebraic equations with the same numbers of unknowns. In the present study, Newton–Raphson iterative method is employed to provide solution for the system of non-linear algebraic equations. Although the method is well known, but for the sake of completeness, a description of the method is presented here for a system of two non-linear equations; the same procedure is adopted to solve the system of $5(N_r\times N_\theta)$ non-linear algebraic equations of the annular sector plate.

The following set of equations is considered:

$$f(x,y)=0,$$
$$g(x,y)=0, \tag{24}$$

where $f(x,y)$ and $g(x,y)$ are two general non-linear equations. Assuming that $(x=r,\ y=s)$ represents a root of the equations, and (x_i,y_i) are an initial guesses in the vicinity of the root; a Taylor series for the set of Eqs. (24) may be expanded about the point (x_i,y_i) as follows:

$$f(r,s)=0=f(x_i,y_i)+\frac{\partial f(x_i,y_i)}{\partial x}(r-x_i)+\frac{\partial f(x_i,y_i)}{\partial y}(s-y_i)+\ldots,$$
$$g(r,s)=0=g(x_i,y_i)+\frac{\partial g(x_i,y_i)}{\partial x}(r-x_i)+\frac{\partial g(x_i,y_i)}{\partial y}(s-y_i)+\ldots. \tag{25}$$

By cutting the series, the following linear equations are obtained:

$$\begin{bmatrix}\frac{\partial f(x_i,y_i)}{\partial x} & \frac{\partial f(x_i,y_i)}{\partial y}\\ \frac{\partial g(x_i,y_i)}{\partial x} & \frac{\partial g(x_i,y_i)}{\partial y}\end{bmatrix}\begin{bmatrix}\Delta x_i\\ \Delta y_i\end{bmatrix}=\begin{bmatrix}-f(x_i,y_i)\\ -g(x_i,y_i)\end{bmatrix}, \tag{26}$$

where $\Delta x_i=r-x_i$ and $\Delta y_i=s-y_i$. The values of Δx_i and Δy_i can be obtained from the system of linear equations (26). By adding $(\Delta x_i,\Delta y_i)$ to the initial guesses (x_i,y_i) another point nearer the root can be obtained as:

$$\begin{bmatrix}x_{i+1}\\ y_{i+1}\end{bmatrix}=\begin{bmatrix}\Delta x_i\\ \Delta y_i\end{bmatrix}+\begin{bmatrix}x_i\\ y_i\end{bmatrix}, \tag{27}$$

where (x_{i+1},y_{i+1}) are modified guesses and are used instead of (x_i,y_i) for the second iteration. The above procedure is repeated until a point which is sufficiently close to the root is obtained. Finally, it should be pointed out that for analysis of plates partially rested on foundation, the foundation parameters k_f and g_f are present only for those grid points rested on foundation, however, for the other grid points at the middle part of the plate k_f and g_f are considered to be zero.

3. Numerical results and discussions

3.1. Verification

In order to demonstrate the accuracy and validity of the results, several comparison studies are carried out. First, the accuracy of the method for plates on foundation is demonstrated. Due to lack of study on bending analysis of annular sector plate resting on foundation, isotropic square plates with side a resting on Pasternak foundation are considered. For the purpose of changing the geometry of an annular sector plate to a square plate, the following large radii and small angle are assumed:

$$a=r_o-r_i,$$
$$\alpha=\frac{a}{\frac{r_o+r_i}{2}}. \tag{28}$$

The linear non-dimensional deflections and moment resultants at the middle point of the square plates with different boundary conditions are tabulated in Table 1. The non-dimensional quantities used in this table are as follows:

$$W^*=\frac{wD}{P_z a^4}\times 10^3;\qquad M^*_{x,y}=\frac{M_{x,y}}{P_z a^2}\times 10^2;$$
$$K_F=\frac{a^4k_f}{D};\qquad G_F=\frac{a^2g_f}{D}, \tag{29}$$

where D is the plate flexural rigidity defined as $D=Eh^3/12(1-\nu^2)$ and Poisson's ratio is $\nu=0.3$. It should be noted that the results reported in Table 1 are for square plates with thickness-to-side ratio $h/a=0.2$, also the non-dimensional foundation parameters are assumed to be $K_F=625$ and $G_F=20$. The validity of the results can be concluded from this table. Furthermore, it can be seen that the convergence of deflection is faster than moment resultant, that is using relatively small number of grid points of 11×11 is sufficient to provide reasonably accurate results for deflection.

In order to demonstrate the accuracy of the results in non-linear analysis, an isotropic solid sector plate (i.e., $r_i=0$) with $\alpha=\pi/3$ subjected to various values of pressures is considered. Non-linear deflections as well as moment and stress resultants at point $(r-r_i)/(r_o-r_i)=0.647$ and $\theta=\pi/6$ of the plate for two values of h/r_o are compared with those reported by earlier researchers [29,23] in Tables 2–6. Due to the fact that in the GDQ method, positions of the grid points are the roots of Chebyshev polynomials; finding response of the plate at $(r-r_i)/(r_o-r_i)=0.647$ is not straightforward. Therefore, the reported deflections

Table 1
Convergence and validity of deflections and moment resultants at the middle point for linear bending analysis of a square plate resting on Pasternak foundation with $K_F = 625$ and $G_F = 20$.

Grid point	CCCC		SSSS		SCSC		
	W^*	$M_x^* = M_y^*$	W^*	$M_x^* = M_y^*$	W^*	M_x^*	M_y^*
5×5	0.8886	1.0874	1.0926	1.1234	0.9785	1.0436	1.1624
7×7	0.8368	0.7662	1.0879	0.9174	0.9472	0.7920	0.8745
9×9	0.8366	0.7687	1.0910	0.9316	0.9484	0.8031	0.8781
11×11	0.8368	0.7722	1.0911	0.9319	0.9485	0.8042	0.8807
13×13	0.8368	0.7720	1.0911	0.9319	0.9485	0.8041	0.8805
15×15	0.8368	0.7721	1.0911	0.9319	0.9485	0.8041	0.8805
17×17	0.8368	0.7722	1.0911	0.9319	0.9485	0.8041	0.8805
[13]	0.8368	0.7722	1.0911	0.9319	0.9485	0.8041	0.8805

Table 2
Comparison of deflections at ($r = 0.647$, $\theta = \pi/6$) for non-linear bending analysis of isotropic solid sector plates.

$\frac{P_z r_o^4}{Eh^4}$	w/h					
	$h/r_o = 0.05$			$h/r_o = 0.1$		
	Present	[23]	[29]	Present	[23]	[29]
100	0.32485	0.32484	0.36010	0.39396	0.39401	0.45760
200	0.57876	0.57860	0.62920	0.66719	0.66701	0.75440
300	0.77136	0.77103	0.83100	0.86203	0.86158	0.96290
400	0.92446	0.92389	0.99190	1.01328	1.01249	1.12460
500	1.05149	1.05078	1.12600	1.13757	1.13652	1.25800

Table 3
Comparison of radial moment resultants at ($r = 0.647$, $\theta = \pi/6$) for non-linear bending analysis of isotropic solid sector plates.

$\frac{P_z r_o^4}{Eh^4}$	$M_r r_o^2/(Eh^4)$					
	$h/r_o = 0.05$			$h/r_o = 0.1$		
	Present	[23]	[29]	Present	[23]	[29]
100	0.96621	0.95753	0.949	0.93977	0.91313	0.881
200	1.66036	1.64170	1.586	1.51291	1.47220	1.383
300	2.13281	2.10337	2.012	1.89318	1.82196	1.711
400	2.48533	2.43229	1.959	2.15794	2.06698	1.959
500	2.74479	2.68104	2.564	2.36303	2.25343	2.160

Table 4
Comparison of circumferential moment resultants at ($r = 0.647$, $\theta = \pi/6$) for non-linear bending analysis of isotropic solid sector plates.

$\frac{P_z r_o^4}{Eh^4}$	$M_\theta r_o^2/(Eh^4)$					
	$h/r_o = 0.05$			$h/r_o = 0.1$		
	Present	[23]	[29]	Present	[23]	[29]
100	1.03059	1.01757	1.058	0.99041	0.96363	1.066
200	1.76928	1.74793	1.772	1.60937	1.55517	1.652
300	2.27852	2.24375	2.253	2.00694	1.92614	2.027
400	2.65325	2.59922	2.305	2.29229	2.18652	2.305
500	2.93631	2.86978	2.877	2.51416	2.38495	2.527

for example are obtained, by passing a polynomial through the deflection of each nodes, and finding the value of that polynomial at $(r - r_i)/(r_o - r_i) = 0.647$. From Tables 2–6 it can be concluded that, prediction of GDQ method for non-linear responses of the isotropic plates are in a close agreement with those reported by Refs. [29,23].

Owing to lack of data in the open literature for non-linear bending analysis of RFG annular sector plates, a comparison study with the finite element code ABAQUS is carried out. A thin RFG annular sector plate with $\alpha = \pi/3$, $r_i/r_o = 1/2$, $n = 3$ and the material properties given in Table 7 under uniform pressure $P_z r_o^4/(E_M h^4) = 5000$ is considered. Predictions of FEM as well as GDQ method for non-linear deflections along radial centerline $(r, \alpha/2)$ of the plate are depicted in Fig. 3. It can be concluded from this figure that the results of GDQ method for non-linear

Table 5
Comparison of radial stress resultants at ($r = 0.647$, $\theta = \pi/6$) for non-linear bending analysis of isotropic solid sector plates.

$\frac{P_z r_o^4}{Eh^4}$	$N_r r_o^2/(Eh^3)$					
	$h/r_o = 0.05$			$h/r_o = 0.1$		
	Present	[23]	[29]	Present	[23]	[29]
100	0.68234	0.69078	0.7174	0.95523	0.96666	1.0317
200	2.14115	2.17332	2.197	2.71864	2.74887	2.926
300	3.77432	3.82799	3.830	4.51872	4.56343	4.849
400	5.40029	5.45819	5.447	6.23029	6.28438	6.666
500	6.95269	7.02032	7.011	7.84803	7.90757	8.375

Table 6
Comparison of circumferential stress resultants at ($r = 0.647$, $\theta = \pi/6$) for non-linear bending analysis of isotropic solid sector plates.

$\frac{P_z r_o^4}{Eh^4}$	$N_\theta r_o^2/(Eh^3)$					
	$h/r_o = 0.05$			$h/r_o = 0.1$		
	Present	[23]	[29]	Present	[23]	[29]
100	0.71473	0.71646	0.7000	1.00484	1.00727	0.9424
200	2.25032	2.25075	2.126	2.86236	2.86322	2.562
300	3.94475	3.95698	3.668	4.76065	4.75168	4.172
400	5.66698	5.63052	5.171	6.5665	6.54178	5.688
500	7.29901	7.22635	6.606	8.27380	8.22950	7.111

Table 7
Material properties of metal and ceramic constituent of an annular sector plate [11].

Property	Metal (aluminum)	Ceramic (silicon carbide)
Young's modulus	$E_M = 70$ GPa	$E_C = 427$ GPa
Poisson ratio	$\upsilon_M = 0.3$	$\upsilon_C = 0.17$

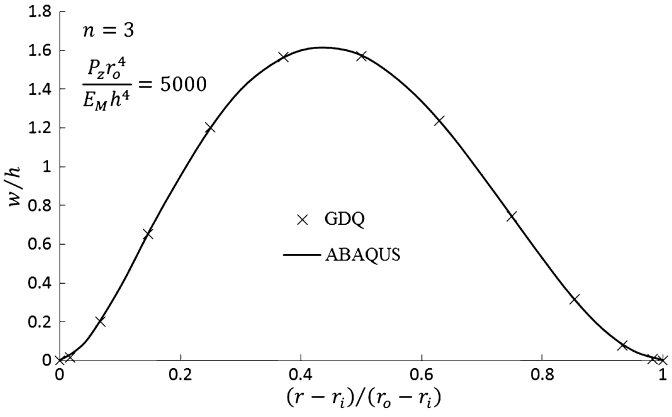

Fig. 3. Non-linear deflection of a thin RFG annular sector plate with $n = 3$ subjected to a uniform pressure.

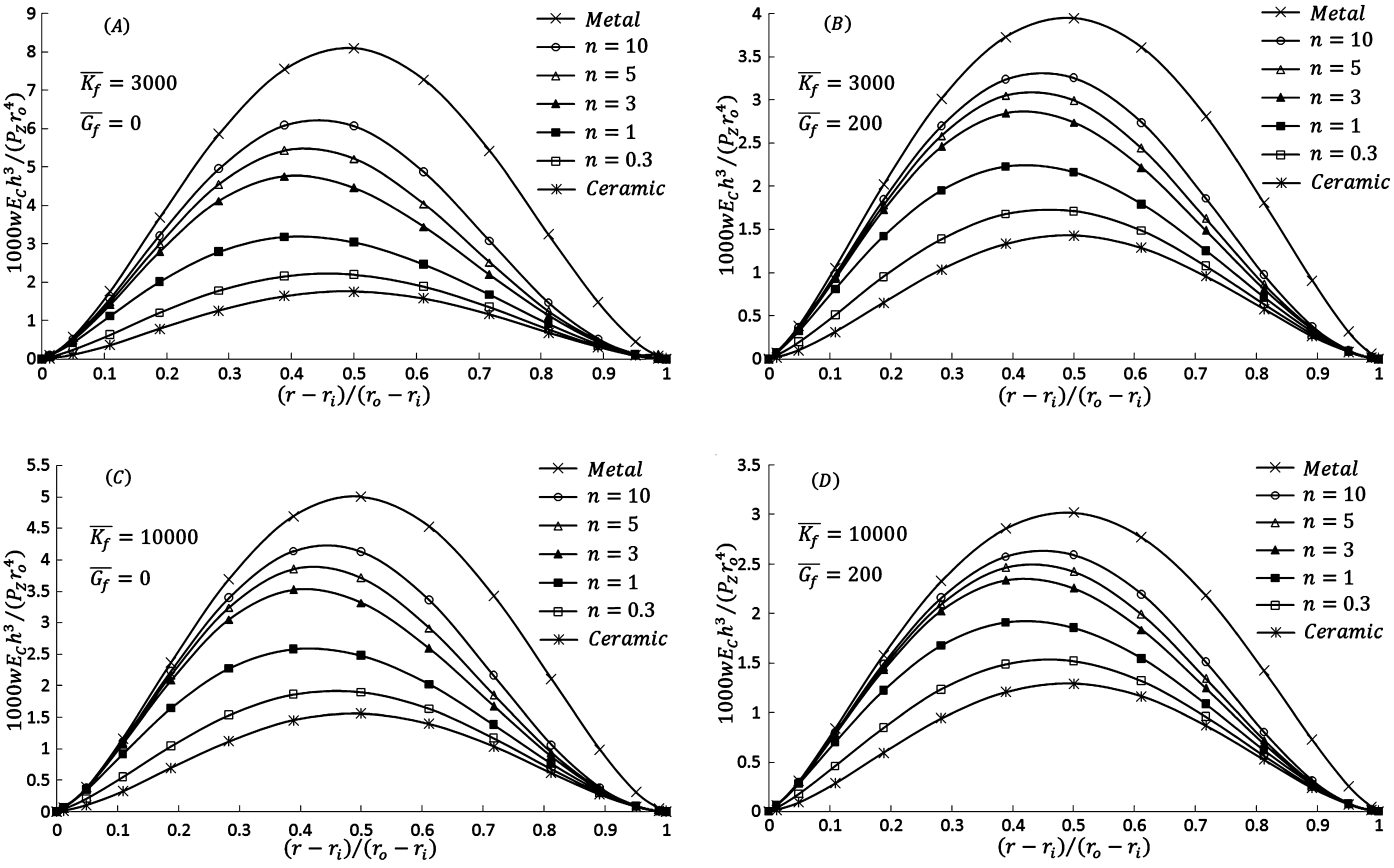

Fig. 4. Linear deflection along radial centerline of RFG annular sector plate rested on foundation.

analysis of RFG annular sector plates are in a good agreement with the prediction of FEM.

3.2. Annular sector plates

Now that the accuracy and validity of the results is demonstrated, the linear and non-linear responses of annular sector plates are investigated in detail. Unless mentioned otherwise, a fully clamped moderately thick RFG annular sector plate with $\alpha = \pi/3$, $h/(r_o - r_i) = 0.1$, $r_i/r_o = 0.5$ and material properties given in Table 7 is considered. Due to the fact that, linear bending analysis of isotropic and RFG annular sector plates rested on foundation is not reported in the open literature; first, linear response of an annular sector plate on foundation is studied. Therefore, non-dimensional linear deflections of the RFG annular sector plate on foundation along radial centerline $(r, \alpha/2)$ for various values of material index and foundation parameters are shown in Fig. 4. The non-dimensional parameters used in this figures are introduced as:

$$\overline{K_f} = \frac{r_o^4 k_f}{D_M}; \qquad \overline{G_f} = \frac{r_o^2 g_f}{D_M}, \tag{30}$$

where D_M is defined as $D_M = E_M h^3/(12(1 - \nu_M^2))$. It can be inferred from Fig. 4 that plates with larger material index exhibit higher deflection as the volume fraction of ceramic reduces by increasing the values of material index. Moreover, it can be seen that, by increasing the foundation parameters deflections of the plates decrease. Furthermore, the effect of raising the foundation shear parameter $\overline{G_f}$ on reduction of the deflection is more than that of increasing the foundation normal parameter $\overline{K_f}$. The effect of foundation on reduction of deflection of plates with larger material index is more than that of plates with smaller material index; hence, the distance between the two displacements curves of ceramic and metallic plates decrease as the values of foundation parameters increase. In addition, the maximum deflection of the plates, especially the RFG plates, does not occur at the middle of the plate i.e., $((r_o + r_i)/2, \alpha/2)$, and the maximum deflection tends to be nearer to the inner radius where the metal constituent is more than the ceramic one.

Non-linear deflections along the radial centerline $(r, \alpha/2)$ of annular sector plates subjected to uniform pressure of $(P_z r_o^4)/(E_M h^4) = 9000$ and for various values of $\overline{K_f}$ and $\overline{G_f}$ are shown in Fig. 5. The results presented in these figures are obtained from the non-linear analysis for plates with different combinations of clamped and simply supported boundary conditions (i.e., CCCC, SSSS, SCSC, CSCS). It is to be mentioned that each of these letters, respectively, represent the clamped (C) or simply supported (S) conditions at the edges of (r_i, θ), $(r, 0)$, (r_o, θ), and (r, α). Since the effect of changing Poisson's ratio on mechanical behavior of FG plates is negligible [7,8], in analysis of annular sector plates with SSSS, SCSC and CSCS boundary conditions, Poisson's ratio is assumed to be constant and equal to 0.3. The elasticity modulus of the FG plates are according to Table 7. As expected, it is seen from the results that deflections of fully simply supported plates are higher than plates with other boundary conditions. Likewise to previous results for linear analysis, maximum deflection of the plate does not occur at the middle of the plate $((r_o + r_i)/2, \alpha/2)$ and this condition for the RFG annular sector plate is more significant. In addition, the deflection of the plate increases by increasing the value of material index n. Moreover, these results show that raising of the foundation shear parameter $\overline{G_f}$ is more effective on reduction of the deflection vis-à-vis increasing of the foundation normal parameter $\overline{K_f}$.

Effects of thickness as well as pressure, on non-linear response of the annular sector plate are studied in Fig. 6. These figures show

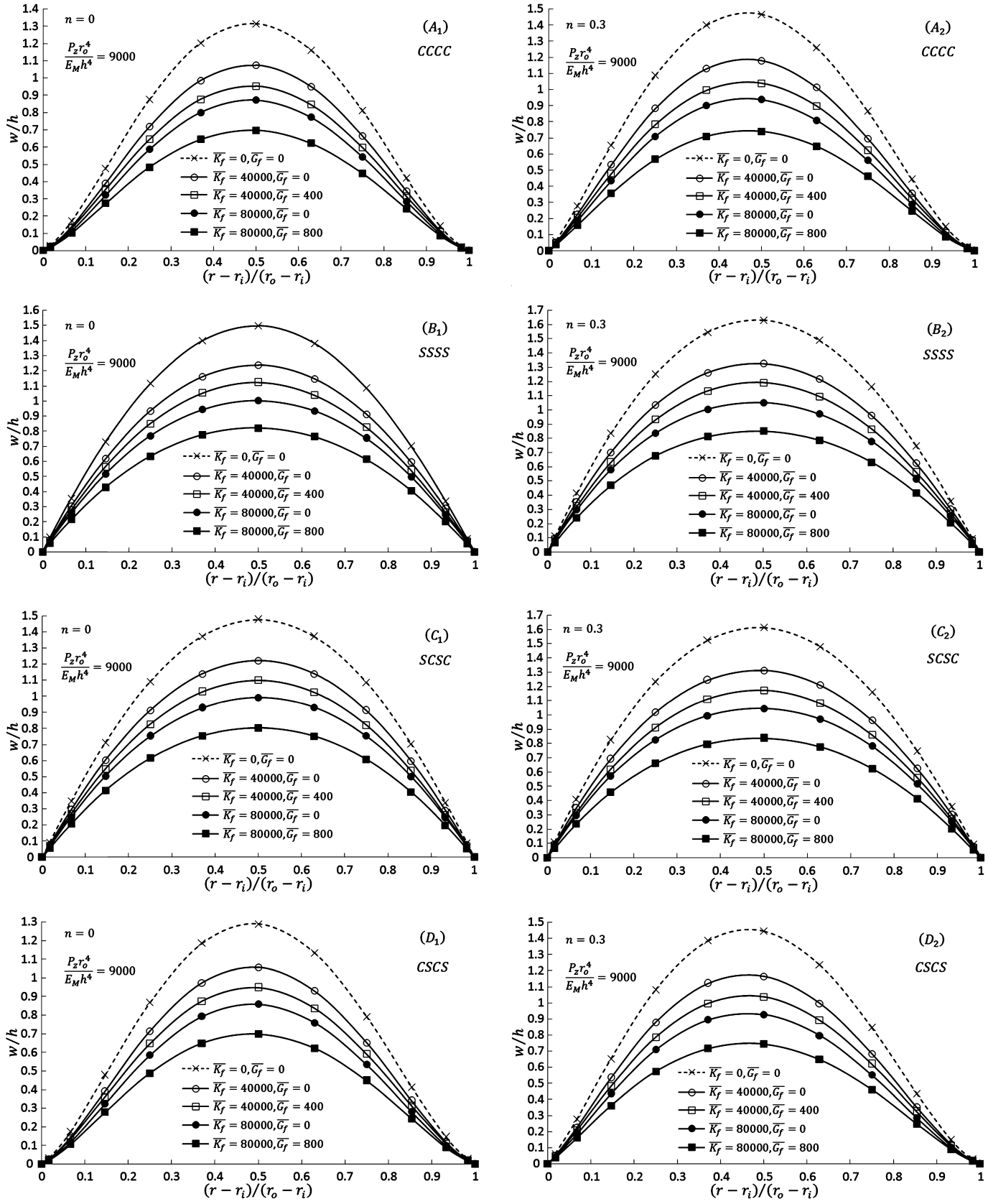

Fig. 5. Non-dimensional deflection along radial centerline for non-linear bending of isotropic and RFG annular sector plate resting on foundation with various foundation parameters.

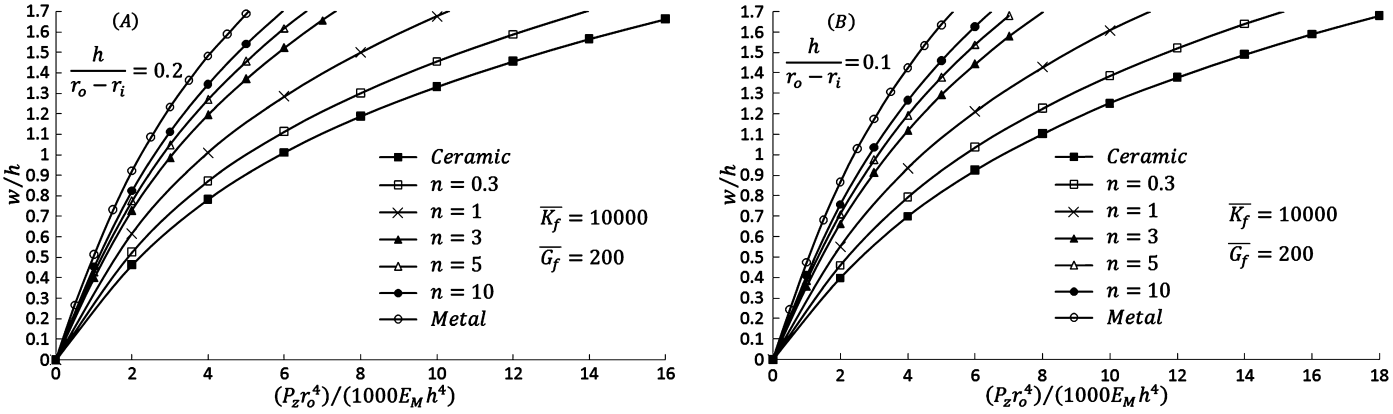

Fig. 6. Non-linear middle point deflection versus pressure for RFG annular sector plates with $h/(r_o - r_i) = 0.1$ and $h/(r_o - r_i) = 0.2$ rested on Pasternak foundation.

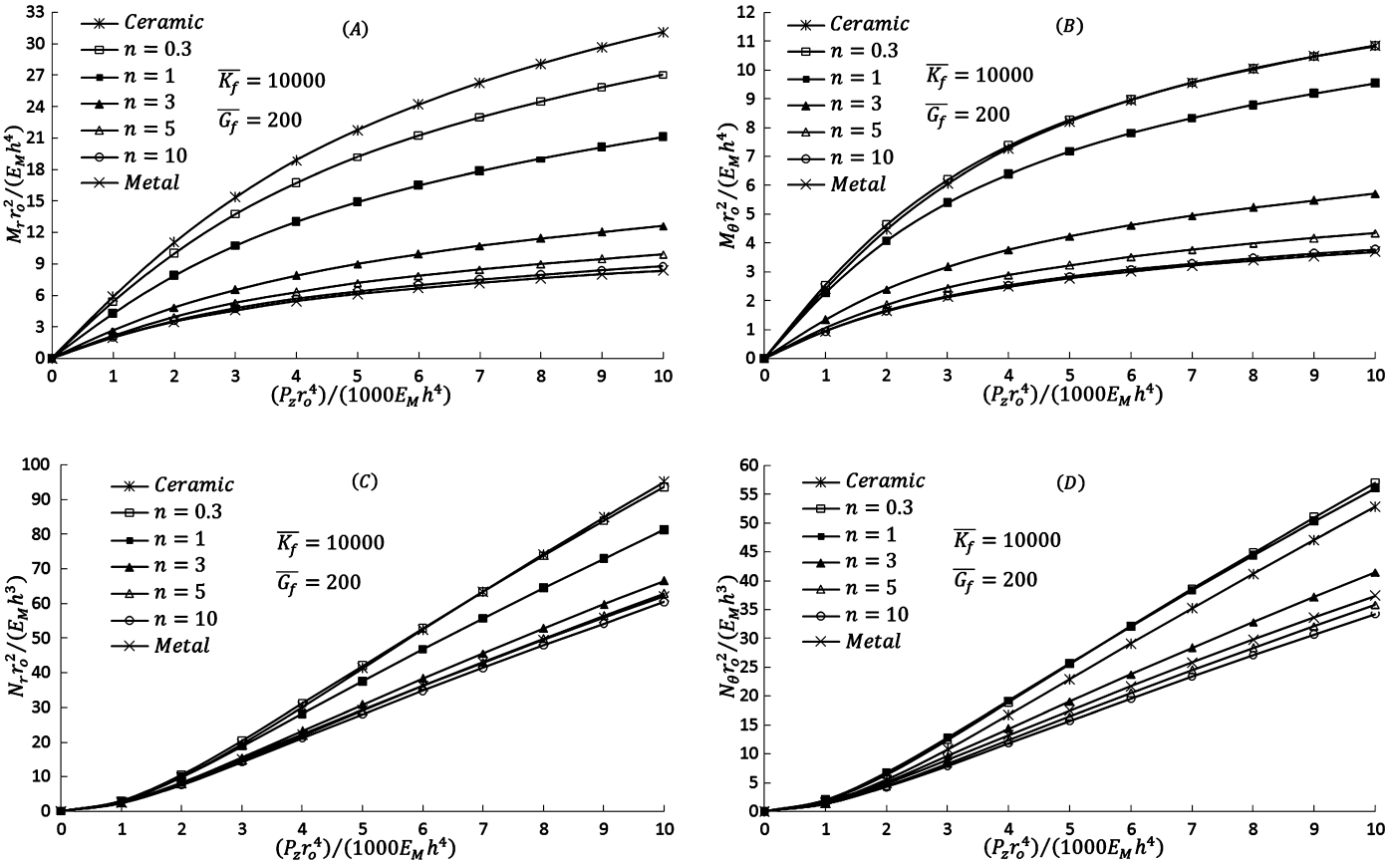

Fig. 7. Moment and stress resultant at the middle point $((r_o + r_i)/2, \alpha/2)$ versus pressure for non-linear bending of RFG annular sector plates resting on Pasternak foundation.

non-dimensional deflections at the middle point $((r_o + r_i)/2, \alpha/2)$ versus dimensionless pressure for non-linear bending of annular sector plates rested on Pasternak foundation with $h/(r_o - r_i) = 0.2$ and $h/(r_o - r_i) = 0.1$. Non-dimensional foundation parameters are $\overline{K_f} = 10\,000$ and $\overline{G_f} = 200$. It has to be pointed out that these deflections are not the maximum deflections of the plates, because the maximum deflection of a RFG annular sector plate does not occur at the middle of the plate. As expected, the obtained results show that by decreasing the plate thickness $h/(r_o - r_i)$, the non-dimensional deflections at the middle of the plate decrease. Moreover, because of more stiffness of ceramic in comparison with metal, plates with larger values of material index show more deflections than those of less index values.

In addition, moment and stress resultants at the middle of plate $((r_o + r_i)/2, \alpha/2)$ versus pressure for non-linear bending of the RFG annular sector plate on Pasternak foundation with $h/(r_o - r_i) = 0.1$ are depicted in Fig. 7. It can be seen that, as the values of material index n increase radial and circumferential moment resultants decrease. Moreover, the effects of raising pressure on radial moment and radial stress resultants are more than those of circumferential moment and circumferential stress resultants. Furthermore, variations of moment resultants with pressure tend to be linear for small values of pressure. Similarly, variations of stress resultants are almost linear for large values of pressure.

3.3. Solid sector plates

RFG solid sector plates (i.e., $r_i = 0$) with $h/r_o = 0.1$ subjected to a uniform pressure $(P_z r_o^4)/(E_M h^4) = 3000$ are considered. It is assumed that the plates are on the elastic Pasternak foun-

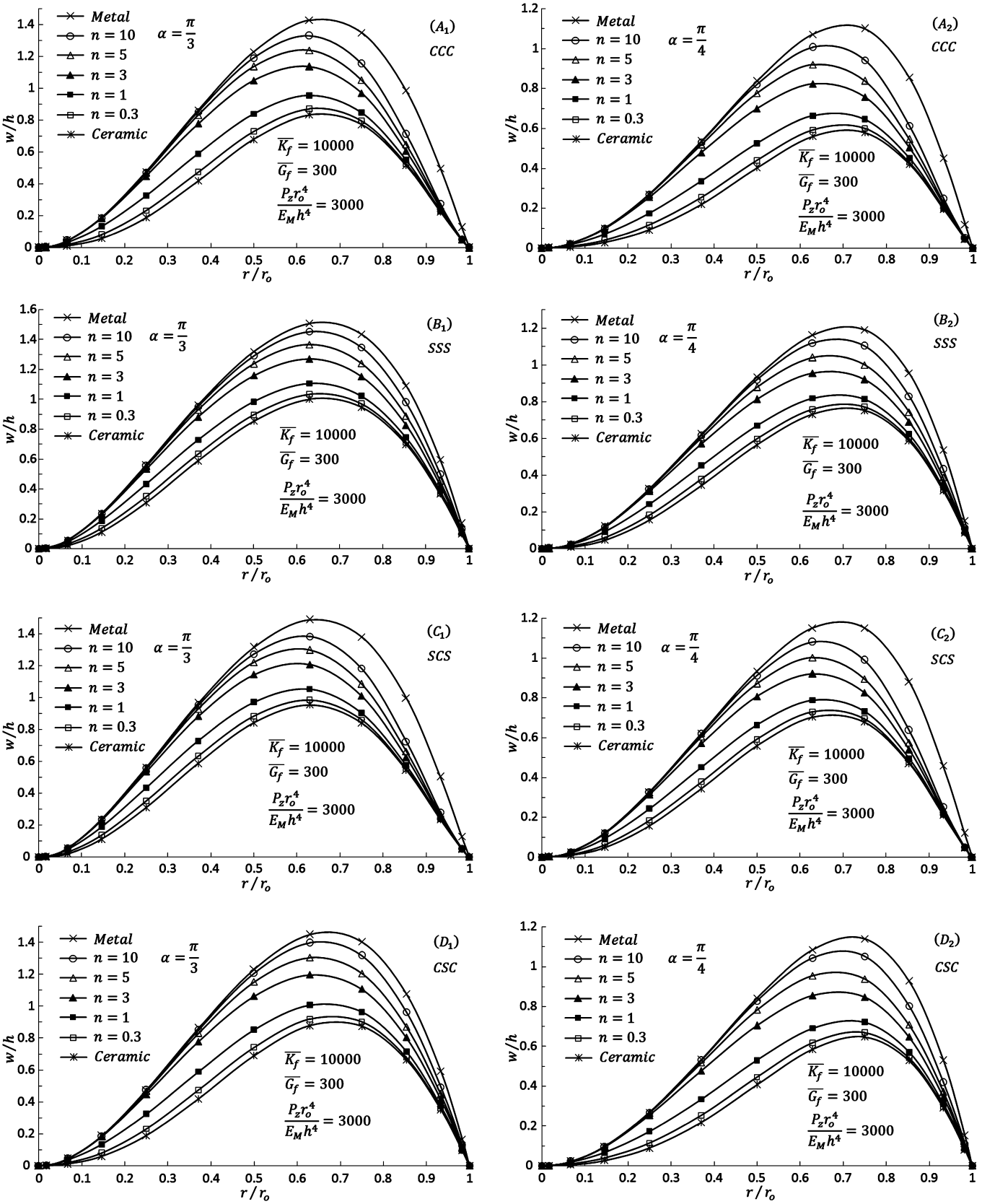

Fig. 8. Effects of sector angle α on non-dimensional deflection along radial centerline for non-linear bending of RFG solid sector plates on the Pasternak foundation.

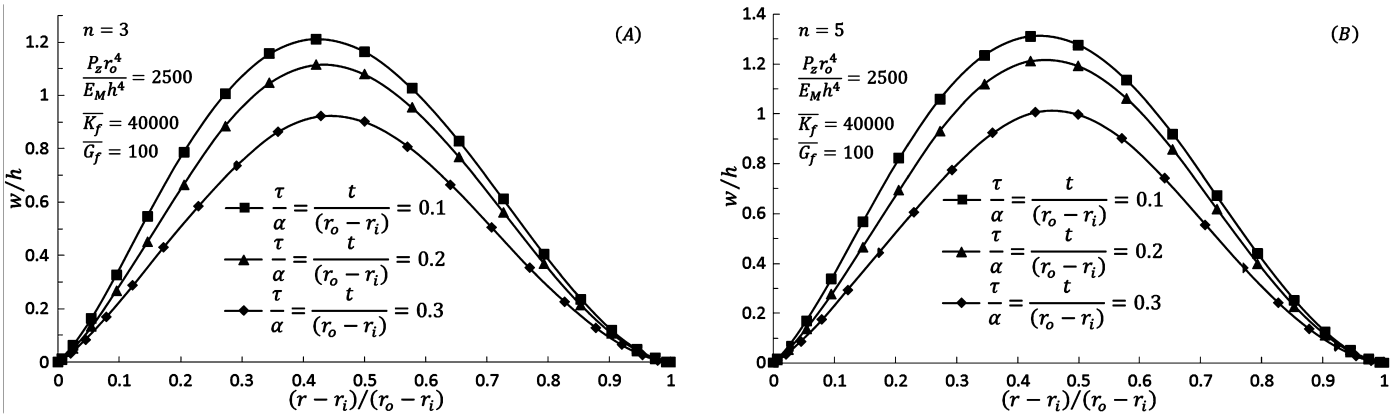

Fig. 9. Non-dimensional deflection along radial centerline for non-linear bending of RFG annular sector plates partially rested on foundation.

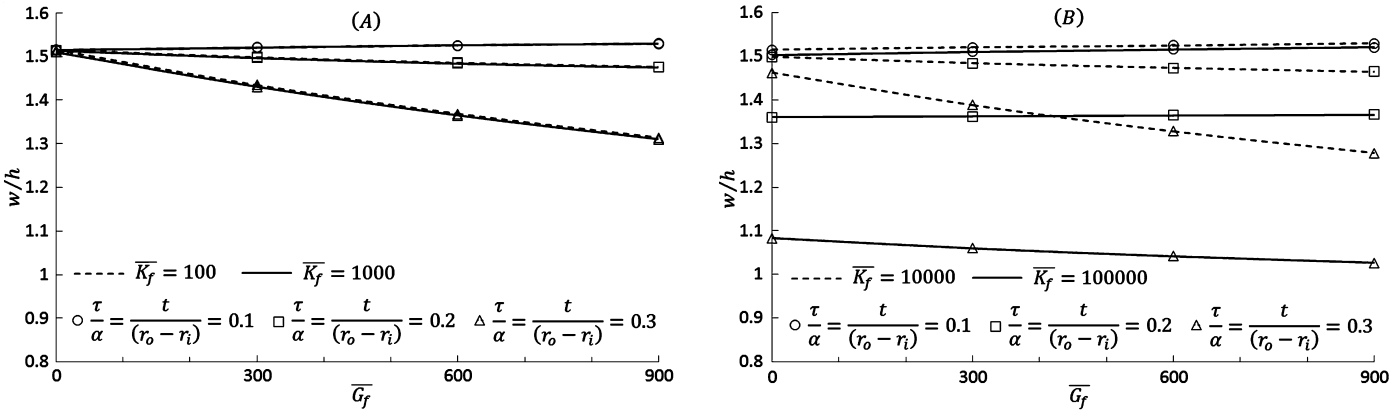

Fig. 10. Non-dimensional deflection at the middle of the plate versus dimensionless foundation shear parameter for non-linear bending analysis of RFG annular sector plates with $n = 2$.

dation with non-dimensional foundation parameters $\overline{K_f} = 10000$ and $\overline{G_f} = 300$. The effects of the angle α on non-linear dimensionless deflections along radial centerline $(r, \alpha/2)$ of the RFG solid sector plates with different combination of clamped and simply supported boundary conditions (i.e., CCC, SSS, SCS and CSC) are studied in Fig. 8. Each letter of the boundary condition specifies the condition at $(r, 0)$, (r_o, θ) and (r, α) edges, respectively. It should be mentioned that the results presented in Fig. 8 are for plates with constant Poisson's ratio of $\nu = 0.3$ and the elasticity modulus of $E_M = 70$ GPa and $E_C = 427$ GPa. As expected, these results show that the solid sector plates display more deflections by increasing the material index n. Furthermore, deflections of the solid sector plates reduce by decreasing the sector angle α. In addition, it can be seen that the maximum deflection of isotropic as well as RFG solid sector plates does not occur at the middle of the plate. Comparing the deflections of isotropic solid sector plate with those of annular one with inner radius r_i, shows that the position of maximum deflection of an isotropic sectorial plate depends on the geometry of the plate, Figs. 5 and 8. However, for a square plate that is a sectorial plate with large radii and small sector angle α, the deflection at the middle of the plate is the maximum deflection.

3.4. Partially foundation

Responses of plates partially rested on foundation are studied in this part. A RFG annular sector plate with $\alpha = \pi/3$, $h/(r_o - r_i) = 0.1$, $r_i/r_o = 0.5$ and material properties given in Table 7 subjected to a uniform pressure of $(P_z r_o^4)/(E_M h^4) = 2500$ is considered. The portion of the plate on foundation along circumferential and radial edges are shown with t and τ, respectively, Fig. 2. In order to create a virtual boundary at $t/(r_o - r_i) = \tau/\alpha = 0.1$ and $t/(r_o - r_i) = \tau/\alpha = 0.2$ to separate the portions of the plate with and without foundations, a mesh of 21×21 grid points is considered. For $t/(r_o - r_i) = \tau/\alpha = 0.3$, a mesh of 23×23 is assumed to perform this separation. Non-dimensional deflections along the radial centerline $(r, \alpha/2)$ for non-linear bending of the RFG annular sector plate partially rested on Pasternak foundation with different values of $t/(r_o - r_i) = \tau/\alpha$ are depicted in Fig. 9. It is seen that deflections of the plates decrease as the foundation covers more portions of the plate. Similar to previous case, increasing the material index cause more deflection.

The effects of foundation parameters on non-linear response of RFG annular sector plates with the geometry and material properties defined in the previous part are studied in Fig. 10. It is assumed that the plates are partially rested on foundations and are subjected to a uniform pressure of $(P_z r_o^4)/(E_M h^4) = 5000$. Fig. 10 shows non-dimensional deflection at $((r_o + r_i)/2, \alpha/2)$ versus the dimensionless foundation shear parameter $\overline{G_f}$ for non-linear bending analysis of RFG annular sector plates with $n = 2$. It can be seen that by increasing the stiffness of the springs $\overline{K_f}$, and for the constant foundation shear parameter, deflections of the plates decrease. However, when $\overline{K_f}$ is constant and $\overline{G_f}$ increases, the deflections increase as it is similarly has been shown by Nobakhti and Aghdam [25].

4. Conclusions

In the present study, large deflection behavior of RFG annular sector plates fully and partially rested on two-parameter elastic foundation was investigated using the GDQ method. The

von Kármán non-linear equilibrium equations of the plates within the first order shear deformation theory were solved using the GDQ method in conjunction with the Newton–Raphson iterative scheme. Several comparison studies were performed to demonstrate the validity and accuracy of the results. Effects of geometric parameters, material index and foundation parameters were investigated in detail and some general observations are summarized as follows:

- The influence of the foundation shear parameter on deflection reduction is more than that of the normal parameter.
- The effect of the foundation on deflection reduction of plates with larger material index is more than that of plates with smaller material index.
- Position and magnitude of maximum deflection depends on the material index as well as the geometry of RFG annular sector plates, i.e., one may obtain customized deflections at a specific position by using proper material distribution and geometric parameters.
- The influences of transverse load on radial moment resultants are more than those of circumferential ones which also true for radial and circumferential stress resultants.
- By increasing the value of foundation normal parameter $\overline{K_f}$, when the foundation shear parameter $\overline{G_f}$ is constant, the deflections of plate decrease. However, it is not the same when $\overline{K_f}$ is constant and $\overline{G_f}$ increase, and in some cases reverse trends are observed.

Conflict of interest statement

The authors declare no conflict of interest.

References

[1] M.M. Aghdam, M. Mohammadi, V. Erfanian, Bending analysis of thin annular sector plates using extended Kantorovich method, Thin-Walled Struct. 45 (2007) 983–990.

[2] M.M. Aghdam, N. Shahmansouri, M. Mohammadi, Extended Kantorovich method for static analysis of moderately thick functionally graded sector plates, Math. Comput. Simul. 86 (2012) 118–130.

[3] A. Andakhshideh, S. Maleki, M.M. Aghdam, Non-linear bending analysis of laminated sector plates using generalized differential quadrature, Compos. Struct. 92 (2010) 2258–2264.

[4] S.R. Atashipour, A.R. Saidi, E. Jomehzadeh, On the boundary layer phenomenon in bending of thick annular sector plates using third-order shear deformation theory, Acta Mech. 211 (2010) 89–99.

[5] R. Bellman, J. Casti, Differential quadrature and long-term integration, J. Math. Anal. Appl. 34 (1971) 235–238.

[6] C.W. Bert, M. Malik, Differential quadrature method in computational mechanics: a review, Appl. Mech. Rev. 49 (1996) 1–27.

[7] S.H. Chi, Y.L. Chung, Mechanical behavior of functionally graded material plates under transverse load—Part I: analysis, Int. J. Solids Struct. 43 (2006) 3657–3674.

[8] S.H. Chi, Y.L. Chung, Mechanical behavior of functionally graded material plates under transverse load—Part II: numerical results, Int. J. Solids Struct. 43 (2006) 3675–3691.

[9] M. Es'haghi, Accurate approach implementation in vibration analysis of thick sector plates, Int. J. Mech. Sci. 79 (2014) 1–14.

[10] A. Fereidoon, A. Mohyeddin, M. Sheikhi, H. Rahmani, Bending analysis of functionally graded annular sector plates by extended Kantorovich method, Composites, Part B, Eng. 43 (2012) 2172–2179.

[11] A.J.M. Ferreira, R.C. Batra, C.M.C. Roque, L.F. Qian, P.A.L.S. Martins, Static analysis of functionally graded plates using third-order shear deformation theory and a meshless method, Compos. Struct. 69 (2005) 449–457.

[12] Y.C. Fung, P. Tong, Classical and Computational Solid Mechanics, World Scientific, New Jersey, 2001.

[13] J.-B. Han, K.M. Liew, Numerical differential quadrature method for Reissner/Mindlin plates on two-parameter foundations, Int. J. Mech. Sci. 39 (9) (1997) 977–989.

[14] A. Hasani Baferani, A.R. Saidi, Accurate critical buckling load/temperature of thick annular sector plates, J. Eng. Mech. 138 (6) (2012) 614–630.

[15] F. Hejripour, A.R. Saidi, Nonlinear free vibration analysis of annular sector plates using differential quadrature method, IMECHE, Part C, J. Mech. Eng. Sci. 226 (2012) 485–497.

[16] Sh. Hosseini-Hashemi, H. Akhavan, H. Rokni Damavandi Taher, N. Daemi, A. Alibeigloo, Differential quadrature analysis of functionally graded circular and annular sector plates on elastic foundation, Mater. Des. 31 (2010) 1871–1880.

[17] Sh. Hosseini-Hashemi, H. Rokni Damavandi Taher, H. Akhavan, Vibration analysis of radially FGM sectorial plates of variable thickness on elastic foundations, Compos. Struct. 92 (2010) 1734–1743.

[18] H. Kobayashi, K. Sonoda, Rectangular Mindlin plates on elastic foundations, Int. J. Mech. Sci. 31 (9) (1989) 679–692.

[19] K.M. Liew, J.-B. Han, Z.M. Xiao, H. Du, Differential quadrature method for Mindlin plates on Winkler foundations, Int. J. Mech. Sci. 38 (4) (1996) 405–421.

[20] F.-L. Liu, Rectangular thick plates on Winkler foundation: differential quadrature element solution, Int. J. Solids Struct. 37 (2000) 1743–1763.

[21] S.M. Mousavi, M. Tahani, Analytical solution for bending of moderately thick radially functionally graded sector plates with general boundary conditions using multi-term extended Kantorovich method, Composites, Part B, Eng. 43 (3) (2012) 1405–1416.

[22] A. Naderi, A.R. Saidi, Exact solution for stability analysis of moderately thick functionally graded sector plates on elastic foundation, Compos. Struct. 93 (2011) 629–638.

[23] Y. Nath, H.B. Sharda, A. Sharma, Non-linear analysis of moderately thick sector plates, Commun. Nonlinear Sci. Numer. Simul. 10 (2005) 765–778.

[24] T.-K. Nguyen, K. Sab, G. Bonnet, First-order shear deformation plate models for functionally graded materials, Compos. Struct. 83 (2008) 25–36.

[25] S. Nobakhti, M.M. Aghdam, Static analysis of rectangular thick plates resting on two-parameter elastic boundary strips, Eur. J. Mech. A, Solids 30 (2011) 442–448.

[26] J.N. Reddy, Energy Principles and Variational Methods in Applied Mechanics, John Wiley and Sons Inc., New York, 1984.

[27] J.N. Reddy, Theory and Analysis of Elastic Plates, Taylor & Francis, Philadelphia, 1999.

[28] A.R. Saidi, E. Jomehzadeh, S.R. Atashipour, Exact analytical solution for bending analysis of functionally graded annular sector plates, Int. J. Eng. Trans. A 22 (3) (2009) 307–316.

[29] M. Salehi, A. Shahidi, Large deflection analysis of elastic sector Mindlin plates, Comput. Struct. 52 (5) (1994) 987–998.

[30] C. Shu, Differential Quadrature and Its Application in Engineering, Springer, London, 2000.

[31] C. Shu, B.E. Richards, Application of generalized differential quadrature to solve two-dimensional incompressible Navier–Stokes equations, Int. J. Numer. Methods Fluids 15 (1992) 791–798.

[32] M. Yamanoushi, M. Koizumi, T. Hiraii, I. Shiota (Eds.), Proceedings of the First International Symposium on Functionally Gradient Materials, Japan, 1990.